Catalysts **2015**, *5*, 718-746; doi:10.3390/catal5020718

OPEN ACCESS

catalysts

ISSN 2073-4344

www.mdpi.com/journal/catalysts

Review

Abatement of VOCs with Alternate Adsorption and Plasma-Assisted Regeneration: A Review

Sharmin Sultana *, Arne M. Vandenbroucke, Christophe Leys, Nathalie De Geyter and Rino Morent

Department of Applied Physics, Research Unit Plasma Technology, Faculty of Engineering and Architecture, Ghent University, Sint-Pietersnieuwstraat 41, B-9000 Ghent, Belgium;
E-Mails: ArneM.Vandenbroucke@UGent.be (A.M.V.); Christophe.Leys@UGent.be (C.L.); Nathalie.DeGeyter@UGent.be (N.G.); Rino.Morent@UGent.be (R.M.)

* Author to whom correspondence should be addressed; E-Mail: Sharmin.Sultana@UGent.be; Tel.: +32-9-264-3838; Fax: +32-9-264-4198.

Academic Editor: Jean-François Lamonier

Received: 26 February 2015 / Accepted: 9 April 2015 / Published: 23 April 2015

Abstract: Energy consumption is an important concern for the removal of volatile organic compounds (VOCs) from waste air with non-thermal plasma (NTP). Although the combination of NTP with heterogeneous catalysis has shown to reduce the formation of unwanted by-products and improve the energy efficiency of the process, further optimization of these hybrid systems is still necessary to evolve to a competitive air purification technology. A newly developed innovative technique, *i.e.*, the cyclic operation of VOC adsorption and NTP-assisted regeneration has attracted growing interest of researchers due to the optimized energy consumption and cost-effectiveness. This paper reviews this new technique for the abatement of VOCs as well as for regeneration of adsorbents. In the first part, a comparison of the energy consumption between sequential and continuous treatment is given. Next, studies dealing with adsorption followed by NTP oxidation are reviewed. Particular attention is paid to the adsorption mechanisms and the regeneration of catalysts with in-plasma and post-plasma processes. Finally, the influence of critical process parameters on the adsorption and regeneration steps is summarized.

Keywords: non-thermal plasma; volatile organic compound; plasma-catalysis; adsorption; regeneration

---

1. Introduction

Air quality issues have become a huge concern of environmental legislation as a consequence of growing awareness in our global world. Exhausts, form outdoor sources (various chemical industries, painting and printing industries, cars) [1] as well as from indoor sources [2], pollute the air with a variety of harmful substances like volatile organic compounds (VOCs) which pose a threat to human health and the environment [3]. The European legislation related to the reduction of volatile organic compounds (VOCs) emission is getting stringent due to their potential toxicity, carcinogenicity and mutagenicity [4,5]. Furthermore, they are also responsible for odor nuisance, the creation of tropospheric ozone leading to photochemical smog, the intensification of global warming and the depletion of stratospheric ozone layer [3]. Therefore, in order to minimize these adverse effects, indoor air cleaning and end-of-pipe (EOP) treatment using various techniques for the abatement of VOCs is becoming most attractive.

Non-thermal plasma (NTP) technology has attracted growing interest of scientists over the last two decades due to its distinctive characteristic of providing a highly chemical reactive environment (e^-, O*, HO_2*, OH*, N_2*, O_3, *etc.*) to decompose VOCs at ambient conditions, which repudiates the use of expensive vacuum systems [6,7]. Although other commercial pollution control techniques (thermal incineration, catalytic oxidation, adsorption, biofiltration) [8] are very efficient for the removal of VOCs, these are energetically expensive and difficult to operate in case of moderate flow rates with low VOC concentration in contrast to NTP [9–12]. In a NTP, electrons with high kinetic energies (1–10 eV) are selectively produced consuming almost all the electric energy supplied to the system instead of heating the entire gas unlike thermal and catalytic oxidation. Collisions of these energetic electrons with neutral background molecules close to room temperature, generate active species such as free radicals, metastables, ions and secondary electrons through different chemical processes such as dissociation, excitation and ionization. These active species are able to decompose pollutant molecules to less harmful products (CO_2, H_2O, H*X* and X_2 with *X* being a halogen) Additionally, the abatement of low concentrated VOCs (up to 1000 ppm), feasible in indoor air treatment application, is challenging for conventional methods because when the VOC concentrations decrease, the cost per unit pollutant treatment becomes higher in comparison to NTP. Furthermore, NTP systems have several desirable features resulting from their operating conditions, such as a quick start-up, compact system, rapid response to changes in the composition of the waste gas and non-selectivity for the treatment of waste gases with different pollutants such as particulate matters, bacteria and VOCs [13–15].

Unfortunately, industrial implementation of NTP for VOC abatement is impaired by three main bottlenecks such as poor product selectivity, formation of undesired by-products (O_3, NO_x, other VOCs, aerosols) that often increase the overall toxicity of the treated gas stream and low energy efficiency. In order to overcome these limitations, many attempts have been made and have engendered the development of a hybrid system using multiple techniques such as packed bed NTP reactors [16,17], NTP/electrostatic precipitation [18], NTP/catalysis [19,20], photocatalysis [21] and adsorption/NTP [22]. Among these VOC removal techniques, the combination of non-thermal plasma with catalysts/sorbents, *i.e.*, plasma-catalysis, is remarkably investigated during the last decade because of their improved performance such as increased energy efficiency and suppressed unwanted

by-products distribution for VOC decomposition. In such a hybrid system, the catalyst can be integrated either inside (IPC-Inside Plasma Catalysis) [23] or downstream (PPC-Post Plasma Catalysis) [24,25] of the discharge region. In both cases a synergetic effect has been reported in many studies [26–28].

Activation of catalyst by the NTP is expected to play an important role in the synergetic effect. There are different possible activation mechanisms ranging from UV, ozone, work function changes, lattice oxygen activation, heating at local spot, adsorption/desorption, electron-hole pair creation and gas-phase radicals which directly interact with adsorbed pollutants [29]. The abatement of VOCs by combined use of NTP and catalysis is not only governed by gas phase reactions but also by surface reactions on the catalyst. Indeed, by introducing a catalyst in the discharge zone, the discharge gap shortens causing an intensification of the electric field strength. This increases the electron density and mean energy, which increases the concentration of active plasma species, hence promoting high VOC removal efficiency. Furthermore, the introduction of a catalyst inside the plasma can change the nature of the discharge itself. Malik *et al.* reported that volume streamers could change into surface streamers near catalyst surfaces in case of plasma-driven catalysis IPC [30]. These surface streamers show enhanced ionization, which promotes the decomposition of VOCs. However, higher VOC mineralization is directly related with the surface reactivity of the inserted material [31]. If the catalyst has high adsorption capacity, the residence time and concentration of pollutant will increase. This will result in a higher collision probability between pollutant and active species, which will simultaneously stimulate the removal efficiency and mineralization degree. For instance, Song *et al.* have revealed that with NTP treatment, the removal rate of propane with molecular sieve is significantly higher (85%) than is the case with glass beads (17%) or a ɣ-Al_2O_3 beads (23%) reactor. This was attributed to the higher surface area and smaller pore size of molecular sieve compared to the latter cases, which have weaker adsorption capabilities for propane [32]. On the other hand, partial/soft oxidation of VOCs by active species generated from NTP can significantly enhance the pollutant affinity for the adsorbents [33,34]. During plasma treatment, modification of the VOCs structure can cause an increase of the molecular size of VOCs. It can also modify their chemical nature through formation of new polar functions on molecules which lead to better retention of VOCs on the adsorbents.

Both adsorption and reaction properties of catalysts are used to increase the residence time of VOCs and their reaction probability with active plasma species leading to high mineralization degree [35]. Considering the importance of adsorption in plasma-catalysis, investigation of NTP with the adsorption process has drawn researchers' interest during the last decade. In 1999, an innovative approach, which increased the ratio between deposited energy and treated molecules, was suggested by Ogata *et al.* [31,36]. According to the authors, by using a cycled system of adsorption and NTP discharge, an energy efficient technique can be achieved when operated at optimized intervals. Besides, in comparison to the continuous treatment, the sequential treatment, *i.e.*, adsorption followed by NTP oxidation, is expected to treat waste streams over a wide range of VOC concentrations. In many chemical facilities there is a large variation of VOC concentrations during the operation period. The adsorption step makes this cycled system effective, since energy is not continuously deposited in the treated gas stream, independently of VOC concentration variations. Thus, optimized energy consumption is achieved with this sequential treatment. Furthermore, suppressed formation of harmful inorganic by-products such as CO, O_3 as well as organic by-products is another benefit of this method.

This could also be an effective regeneration technique compared to conventional techniques like thermal treatment, which often leads to catalytic deactivation owing to particle agglomerations on catalyst surfaces and poses high a cost. Recently Thevenet *et al.* have partly reviewed the sequential treatment in their publication [37].

This paper presents an intensive literature review dealing with the abatement of VOCs and regeneration of saturated adsorbents with NTP. In the first part the concept of sequential treatment is discussed. Next, the current status and recent achievements of this new technique for the abatement of VOCs is reviewed. The present understanding of the mechanisms involved in adsorption and oxidation pathways during the regeneration process found in literature are summarized. Finally, the influence of critical process parameters on the adsorption and regeneration step is discussed in detail.

2. Sequential Treatment (Adsorption Followed by NTP Oxidation)

A schematic diagram of a continuous flow process is shown in Figure 1. The IPC process is a single stage process where the catalyst is exposed to the active discharge region. In a dry air ozonolysis (PPC) reactor, the polluted gas stream passes through the plasma discharge followed by the catalytic reactor downstream. In both cases, plasma is ignited permanently and the catalyst material can be incorporated into the hybrid reactor in different ways, for instance, as a coating on reactor walls or electrodes, as a packed bed (powder, pellets, coated fibers or porous solid foam) or a layer of catalyst material (usually powder/pellets) [25].

The conceptual diagram of sequential treatment or cycled storage-discharge (CSD) plasma catalytic process for VOC abatement is shown in Figure 2. Firstly, in the adsorption or storage stage, the polluted air stream passes through the catalyst/sorbent bed so that VOCs are removed from the gas phase by adsorption on the catalyst/sorbent until saturation occurs. Next, the saturated catalyst bed is exposed to plasma to oxidize adsorbed VOCs in the regeneration or discharge stage. During this step, the polluted gas stream can be diverted to a fresh catalyst/sorbent bed to ensure continuous operation. In this cyclic approach, surface reactions between adsorbed VOCs/intermediates and plasma generated species such as O_3 or O radicals on the sorbent are of great importance for the oxidative decomposition of VOCs.

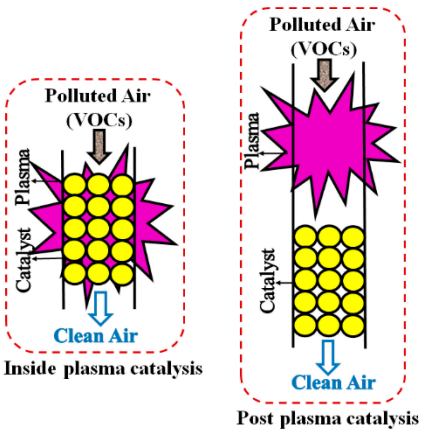

Figure 1. Schematic diagram of continuous plasma-catalysis process.

The energy cost E_c (kWh/m^3) for a sequential treatment is defined as followed:

$$E_c = \frac{P_{\text{discharge}} \times t_2}{F_1 \times t_1} \quad (1)$$

where F_1 is the flow rate (m^3/h) during the storage stage and t_1 and t_2 are the storage and discharge period (h), respectively. In this case, a long storage and a short discharge period are key to achieving low energy cost. The difference in the definition of energy cost between sequential treatment and a continuous flow process is attributed to the energy deposition method. In a continuous flow process, energy density (J/L) *i.e.*, the energy deposited per unit volume of process gas, is required to calculate the energy cost as energy is consumed by the discharge to treat the polluted gas stream. Contrary, in sequential treatment, energy is only alternately deposited during the discharge stage (see Figure 2b). Therefore, the energy consumption for sequential treatment is substantially reduced compared to continuous plasma-catalysis processes. For instance, Sivachandiran *et al.* reported that the energy cost for Isopropanol (IPA-$CH_3CHOHCH_3$) removal using a Mn_xO_y packed bed NTP reactor, is 14.5 times less with the sequential approach compared to a continuous treatment process [38]. Furthermore, to achieve the same mineralization degree, sequential treatment consumes 10 times less energy.

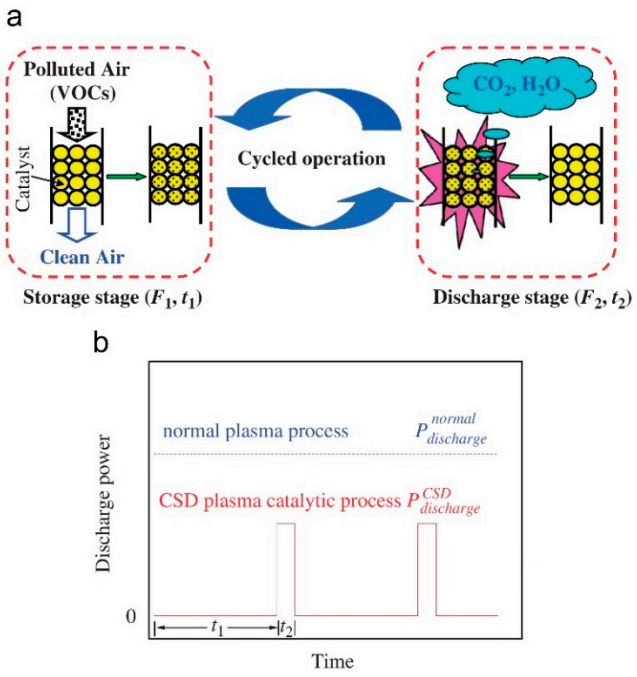

Figure 2. (**a**) Conceptual diagram of sequential treatment, (**b**) difference in discharge power between cycled storage-discharge (CSD) and a continuous plasma catalytic flow process. Reprinted from Ref. [39], with permission from Elsevier.

Since the sequential treatment has gained increased interest over the last decade, an overview of published papers will be given that help to understand the degradation pathway and to optimize the process parameters. Table 1 summarizes the results regarding the adsorption and regeneration stage of these publications found in literature.

Zhao *et al.* have investigated the removal of formaldehyde (HCHO) from air using a CSD plasma catalytic process over AgCu/HZSM-5 (HZSM-5, SiO_2/Al_2O_3 = 360) catalyst for indoor air purification [39]. Their system combined extremely low energy cost with excellent humidity tolerance

while no secondary pollution was detected. In order to achieve 100% conversion of HCHO to CO_2, almost the same discharge period (t_2 = 10 min) was required for different storage periods (t_1 = 100, 300, 600 min). This proves that long storage periods can be employed to achieve low energy cost. It is reported that the energy cost to remove 6.3 ppm of HCHO from humid air reaches 1.9×10^{-3} kWh/m^3. This cost could be further lowered to 10^{-5}–10^{-4} kWh/m^3 by increasing the storage period to purify diluted HCHO (several hundred ppb) in a typical indoor air environment.

Almost complete oxidation of benzene (C_6H_6) as well as extremely low energy cost were also achieved by using an Ag/HZSM-5 catalyst-packed dielectric barrier discharge (DBD) in sequential treatment [40]. The energy cost for sequential treatment of air containing 4.7 ppm benzene was 3.7×10^{-3} kWh/m^3 while 99.8% CO_2 selectivity was achieved. The catalytic effect of Ag to promote CO oxidation to CO_2 and the strong adsorption of Ag with benzene through π-complexation are found to be responsible for this high selectivity [41].

The effect of different catalysts and reactor configurations on plasma catalytic oxidation of stored benzene was also investigated by the same group [42]. The performance of plasma-catalytic oxidation of stored benzene on different metal (Ce, CO, Ag, Mn, Fe, Ni, Cu, Zn) loaded HZSM-5 catalysts was evaluated in terms of carbon balance (B_c) and CO_2 selectivity (S_{CO_2}). Experiments revealed that 0.8 wt.% Ag/HZSM-5 catalyst could significantly improve plasma catalytic oxidation of stored benzene to CO_2 ($X_{(c_6H_6)_s} \rightarrow CO_2 \approx 100\%$) in a very short discharge time while the formation of unwanted by-products was almost completely suppressed (Figure 3). However, further increase of Ag loading decreased the carbon balance. Regarding the effect of reactor configuration, both carbon balance and CO_2 selectivity reached almost 100% with an IPC reactor (C) within 10 min (Figure 3). In contrast, with a PPC reactor (A and B) the stored benzene was not able to be completely oxidized even after a long discharge time.

Wang *et al.* have tested various metal loaded zeolites (Ag/HZSM-5, Mn/HZSM-5, Ce/HZSM-5, Ag-Mn/HZSM-5) to remove low concentration of toluene ($C_6H_5CH_3$) by intermittent use of adsorption and non-thermal plasma regeneration [43]. In this investigation, a link tooth wheel-cylinder DC plasma reactor is placed upstream of the adsorption/catalyst reactor, which is supported by a glass sieve plate. It is suggested that owing to the unique characteristics of the orbitals of Ag or Ag^+, normal σ bonds to carbon as well as bonds with unsaturated hydrocarbons can be formed in a non-classical manner [44], leading to higher adsorption capacity of Ag loaded zeolites (Ag/HZSM-5, Ag-Mn/HZSM-5). Similar to previous studies, reduced energy consumption (2.2×10^{-3} KWh/m^3) is also reported which is related to high adsorption capacity. Experiments reveal that the catalytic activity for toluene conversion is in the order of Ag-Mn/HZSM-5>Mn/HZSM-5>Ag/HZSM-5>Ce-Mn/HZSM-5>Ce/HZSM-5 which is in accordance with their O_3 decomposition ability. Furthermore, it is widely known that oxidation of toluene is significantly affected by lattice oxygen of manganese oxides. Moreover, the ratios of lattice oxygen to surface adsorbed oxygen on the Mn catalysts is enhanced with appropriate Ag loading [45], which explained the high activity and CO_2 selectivity (99.9%) of Ag-Mn/HZSM-5 for toluene decomposition.

Mok *et al.* have tested a ɣ-Al_2O_3 packed DBD reactor for the treatment of toluene in a sequential approach [46]. The removal efficiency reached 71.4% while ozone was the only by-product of toluene oxidation besides CO and CO_2. The energy yield for the treatment of toluene was reported to be 41.2 J/μmol. Experiments revealed that higher discharge power favored formation of CO and CO_2 at shorter discharge period.

Table 1. Overview of published papers on sequential treatment.

Adsorption					Regeneration/NTP Oxidation							
Target pollutant	**Catalyst/Adsorbent**	**Specific surface area (m^2/g)**	**Carrier gas and flow rate (mL/min)**	**Concen-tration (ppm)**	**Plasma reactor type**	**Carrier Gas and flow rate (mL/min)**	**P_{dis} (W) SIE (J/L)**	**Time t (min)**	**Maximum removal efficiency (%)**	**Mineralization rate m (%) CO_2 yield c (%)**	**E_c (kWh/m^3)**	**Ref.**
Acetone (C_3H_6O)	TiO_2	38 ± 3	dry air 1000	180	DBD/IPC	dry air 1000	0.33 W	t_1 = 103 t_2 = 30	27	m = 12 c = 11	-	[47]
					DBD/IPC + TPD				91 [a]	m = 52[a]		
Benzene	Ag/HZSM-5	334	80% N_2 + 20% O_2 (50% RH) 600	4.7	DBD/IPC	O_2 60	4.7 W	t_1 = 840 t_2 = 24	~100	c = 99.8	3.7×10^{-3}	[40]
Toluene	Ag/HZSM-5	-	Air 3000	3	link tooth wheel cylin-der/PPC	synthetic air (40 ± 5% RH) 1000	-	-	62 [a]	c > 90	2.2×10^{-3}	[43]
	Mn/HZSM-5								69			
	Ce/HZSM-5								56 [a]			
	Ce-Mn/HZSM-5								93			
	Ag-Mn/HZSM-5								70 [a]	c = 99.9		
Formalde-hyde	Ag(3.6 wt.%)-Cu(2.1 wt.%)/HZSM-5	229	80% N_2 + 20% O_2 (50% RH) 300	6.8	DBD/IPC	O_2 60	2.3 W	t_1 = 690 t_2 = 10	100	c > 99	1.9×10^{-3}	[39]
Isopropanol	TiO_2	38 ± 3	Air (50% RH) 1000	163	DBD/IPC	air (50% RH) 1000	-	t_1 = 1 30 $t_2 \approx 60$	91	-	-	[35]

Table 1. *Cont.*

Adsorption					Regeneration/NTP Oxidation							
Target pollutant	**Catalyst/Adsorbent**	**Specific surface area (m^2/g)**	**Carrier gas and flow rate (mL/min)**	**Concentration (ppm)**	**Plasma reactor type**	**Carrier gas and flow rate (mL/min)**	**P_{dis} (W) SIE (J/L)**	**Time *t* (min)**	**Maximum removal efficiency (%)**	**Mineralization rate *m* (%) CO_2 yield *c* (%)**	**E_c (kWh/m^3)**	**Ref.**
Benzene	HZSM-5	328	80% N_2 + 20% O_2 (50% RH) 600	4.7	DBD/IPC	O_2 60	4.7 W	t_1 = 60 t_2 = 9	100	c = 89 [a]	-	[42]
	Ag(0.8 wt.%)/HZSM-5	334							100	c = 100		
	Ag(1.9 wt.%)/HZSM-5	329							92 [a]	c = 100		
	Ag(4.2 wt.%)/HZSM-5	306							63	c = 100		
Benzene	Ag(1 wt.%)/TiO_2	≤68	air (50% PP) 4000–5000	200	DBD/IPC	O_2 5000–8000	169 J/L	-	100 [a]	-	-	[29]
	Ag(4 wt.%)/TiO_2		Air (60% PP)				136 J/L		75 [a]	c = 80 [a]		
	0.5%Ag/ɣ-Al_2O_3	≤210					160 J/L		90 [a]	c = 75 [a]		
	H-Y zeolite	≤520	Air (80% PP) 10000				140 J/L		100	c ~64 [a]		
	Ag(2 wt.%)/H-Y zeolite						160 J/L		100	c ~73 [a]		
Formaldehyde	mineral granulate (MP 5)	-	N_2 176	99	DBD/IPC	N_2 57	2.2 W	t_1 = 250 t_2 = 4	94	m = 38.7 [b] c = 26.5 [b]	-	[48]
Acetaldehyde (CH_3CHO)	α-Al_2O_3	14	95% N_2 + 5% O_2 100	1000	corona discharge/IPC	95% N_2 + 5% O_2 100	1 W	-	25	-	-	[49]
Toluene	ɣ-Al_2O_3	237	N_2 2500	-	DBD/IPC	O_2 2500	88 W	t_1 = 190 t_2 = 70	71.4	-	41.2 J/μmol	[46]

Table 1. *Cont.*

Adsorption					Regeneration/NTP Oxidation							
Target pollutant	**Catalyst/ Adsorbent**	**Specific surface area (m^2/g)**	**Carrier gas and flow rate (mL/min)**	**Concen-tration (ppm)**	**Plasma reactor type**	**Carrier gas and flow rate (mL/min)**	**P_{dis} (W) SIE (J/L)**	**Time t (min)**	**Maximum removal efficiency (%)**	**Mineralization rate m (%) CO_2 yield c (%)**	**E_c (kWh/m^3)**	**Ref.**
Isopropanol	Mn_xO_y	16 ± 2	dry air 1000	165	DBD/IPC	dry air 1000	0.82 ± 0.02 W	t_1 = 6 t_2 = 30	66	m = 56 c = 44	-	[50]
					DBD/IPC + TPD				96	m = 84 c = 72		
					DBD/PPC		0.42 ± 0.02 W		41	m = 27 c = 21		
					DBD/PPC + TPD				84	m = 57 c = 51		
Isopropanol	TiO_2	45	dry air 750	98	DBD/PPC	dry air	68.2 mW	t_1 = 130 t_2 = 70	24	m = 2 c = 1.7 [b]	-	[51]
Acetone				175			72 mW			m = 6		
Acetaldehyde	fibrous activated carbon textile	26.32 [b]	air 100	200	ac-neon transformer	-	6 J/cm^2	-	100	-	-	[22]
Toluene	zeolites	-	air 150000	10–120	DBD/IPC	air 150,000	89 W	-	90–39	-	2.6–13 g/kWh	[52]

TPD—Temperature programmed desorption (296-673 K, 0.4 K/s); PP—Partial pressure of O_2, RH- Relative humidity; [a] Approximate value extracted from graphs; [b] Calculated value from equations.

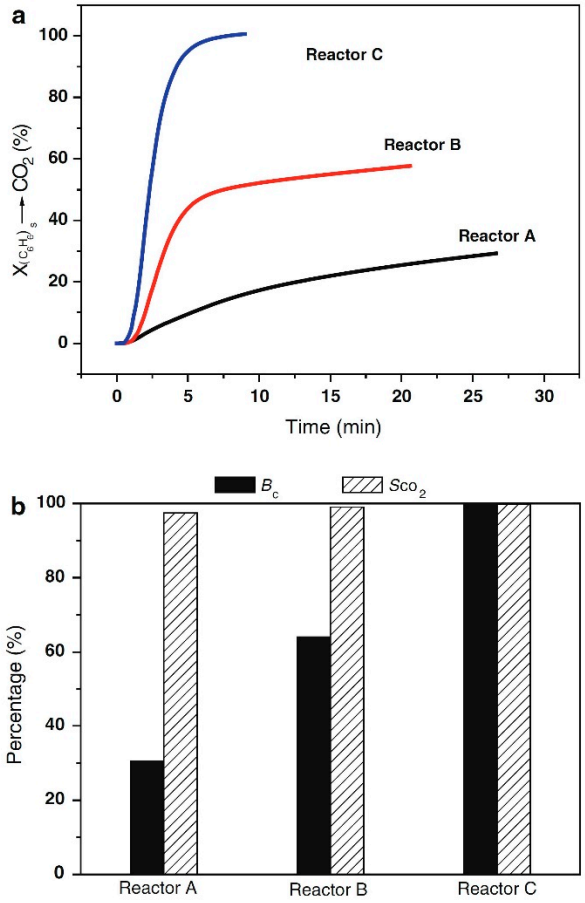

Figure 3. The effect of plasma catalytic reactor configurations on removal of stored benzene over 0.8 wt.% Ag/HZSM-5 catalysts (**a**) the conversion of stored-benzene to CO_2, (**b**) carbon balance and CO_2 selectivity (storage stage with 4.7 ppm benzene, 50% RH (25 °C), 600 mL/min flow rate of simulated air, t_1 = 1 h; discharge stage: 60 mL/min O_2, P = 4.7 W). Reprinted from Ref. [42], with permission from Elsevier.

Kim *et al.* have compared the decomposition of benzene by using flow-type plasma-driven catalysis (IPC) and a cycled system [9]. In the flow type IPC reactor, the formation of N_xO_y is unavoidable and is correlated with the increase of the conversion of VOCs. In contrast, oxygen plasma completely oxidized the adsorbed benzene on 2.0 wt.% Ag/TiO_2 to CO_2 in cycled system, which is impossible with the conventional NTP alone process or the flow-type IPC system.

O_2 plasma treatment as well as O_3 injection were found to be effective for the regeneration of deactivated gold supported TiO_2 surface after exposure to 100 ppm toluene or propylene [53]. IPC configuration showed better oxidation performance of adsorbed toluene than PPC configuration. Adsorbed toluene or propylene was preferentially decomposed to CO_2 in both regeneration methods. In case of PPC configuration, direct reaction between gas phase O_3 and adsorbed toluene instead of desorbed toluene is suggested by the authors as a possible pathway for toluene decomposition.

In order to understand the role of adsorption on the removal of acetaldehyde, Klett *et al.* have used sequential treatment [49]. A wire to cylinder configuration packed with α-Al_2O_3 pellets was used to adsorb 1000 ppm CH_3CHO during the adsorption process. After saturation of the adsorbent it was treated with less than 1 W plasma regenerating only 25% of the saturated adsorbent. In order to

analyze the role of surface reactivity on the possible decomposition pathway, adsorption of multicomponent mixtures of CH_3CHO, CO, CO_2 and O_3 was carried out and the interactions existing between different compounds and the catalyst surface have been identified. Authors have also used diffuse reflectance infrared Fourier transform spectroscopy (DRIFTS) and have detected several intermediates (acetate, formate) during the adsorption step. During the regeneration of saturated alumina with plasma, the DRIFT study revealed both the presence of acetaldehyde and some intermediates on the surface, which are incorporated in the decomposition reaction. Adsorbed oxygen species, resulting from O_3 decomposition on the surface, lead to CH_3CHO decomposition and CO oxidation to CO_2. Clearly, more acetaldehyde was decomposed to CO and CO_2 due to surface reactions than in the gas phase [49].

The regeneration of IPA and acetone saturated TiO_2 surface under O_3 flow produced by NTP (PPC) was investigated by Barakat *et al.* [51]. To elaborate the oxidation mechanism of IPA and acetone, simultaneous analysis of the gas phase and absorbed phase was carried out with Fourier transform infrared spectroscopy (FTIR) and DRIFTS, respectively. The adsorption of IPA on TiO_2 surface leads to the formation of three surface species. The formation of monodentate isopropoxy groups and surface hydroxyl species indicates dissociative adsorption of IPA through Equation (2) [35], where $S_{(1)}$, $S_{(2)}$ represent two different adsorption sites. Strongly bonded IPA species on surface Lewis acid sites ($Ti^{+\delta}$) and weakly hydrogen bonded IPA species on surface basic sites ($Ti^{+\delta}$) are the result of non-dissociative adsorption of IPA on TiO_2 surface. Regarding IPA oxidation, authors reported that O_3 was simultaneously adsorbed on TiO_2 strong Lewis acid sites and on adsorbed IPA (0.2 O_3 molecule per one IPA molecule). Experiments revealed that independently of the adsorption modes, dissociated and non-dissociated IPA on TiO_2 showed the same reactivity with ozone. Only 2% mineralization was achieved (since seven O_3 molecules are required to release one CO or CO_2 in the gas phase) and 22% of the irreversibly adsorbed IPA was desorbed as intermediate by-product acetone. Agreeing with Arsac *et al.* [54], the authors proposed that acetone, produced from oxidation of adsorbed IPA on $S_{(1)}$ sites, could not remain adsorbed on similar adsorption sites (due to competitive adsorption phenomena between IPA and acetone). Acetone either rapidly desorbed to the gas phase if no surface sites denoted by $S_{(2)}$ were available or diffused toward an available $S_{(2)}$ site. Noting that only a small fraction of TiO_2 surface sites $S_{(2)}$ are specific to the acetone adsorption (there is no competitive chemisorption with IPA). For IPA, literature data [54–56] strongly suggest that acetone is the single route to produce CO_2 and H_2O. Experiments have revealed that when the TiO_2 surface is fully saturated with IPA, small amounts of $S_{(2)}$ sites are accessible for irreversibly adsorbed acetone and its subsequent oxidation into CO_2 [51]. Since, for mineralization, adsorbed IPA needs to go through $S_{(2)}$ adsorbed acetone, oxidation of IPA and acetone into CO_2 have the same limiting step.

$$CH_3CHOHCH_3 + S_{(1)} + S_{(2)} \rightarrow S_{(1)}CH_3CHOCH_3^{ads} + S_{(2)} - H^{ads} \quad (2)$$

The regeneration of acetone adsorbed TiO_2 surface has also been conducted with an IPC process by Sivachandiran *et al.* [47]. The NTP regeneration is, however, limited to 30%. During the adsorption stage, 30% of adsorbed acetone is converted into adsorbed mesityl oxides by surface aldolization. These mesityl oxides are fragmented into carboxylic acid (e.g., formic acid) by NTP treatment, which was also evidenced by Barakat *et al.* [51]. It was confirmed that formic acid was poorly sensitive to

NTP treatment but directly converted into CO_2 under successive thermal treatment. Hence, enhanced mineralization can be achieved using the NTP technique followed by thermal treatment [47].

Recently, three different methods have been used by the same group for regeneration of an IPA saturated Mn_xO_y surface [50]. In order to emphasize the proficiency of NTP treatment compared to other regeneration methods, the total carbon mass balances obtained by each method were reported and are shown in Figure 4. Although 94% regeneration efficiency has been achieved with dry air thermal treatment (DTT), 57% of carbon mass balance is accounted for molecularly by desorbed IPA and acetone, which is considered as a drawback. Dry air ozonolysis (PPC) achieved the lowest regeneration efficiency (41%) with 23% CO_x and 12% acetone contribution. *In-situ* NTP (IPC) treatment is considered as the most efficient method to obtain high mineralization and low VOCs desorption, even though 66% of irreversibly adsorbed IPA has been removed. A possible oxidation/mineralization pathway for adsorbed IPA on Mn_xO_y surface by PPC-DTT and IPC treatment was also proposed in Equations (3–7) and (8–10), respectively. Acetaldehyde and isopropyl esters of formic and acetic acids are the main identified intermediate species in both PPC and DTT methods. This indicates the dependency of the adsorbed IPA decomposition pathway on IPA adsorption modes rather than the regeneration methods. In case of IPC treatment, acetone is the main intermediate species. As reported in [51], IPC treatment prior to thermal treatment significantly improves regeneration efficiency and mineralization degree.

Sivachandiran *et al.* have also studied the influence of air humidity on IPA adsorption on TiO_2 surface and surface plasma regeneration efficiency [35]. During this investigation, only 36% regeneration efficiency has been obtained with dry air NTP treatment. Dry air NTP assisted regeneration of IPA saturated Mn_xO_y showed better performance in terms of total carbon mass balance and CO_x selectivity compared to TiO_2 surface [50]. The superior removal/regeneration efficiency of Mn_xO_y metal oxide is ascribed to the higher ability to decompose ozone. These results revealed the importance of surface reactivity of catalyst placed inside the NTP discharge zone.

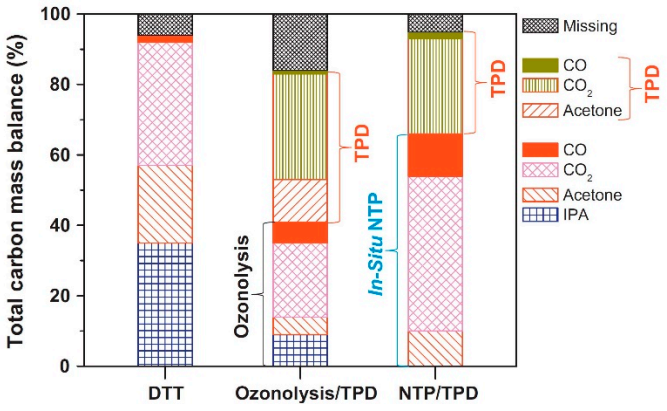

Figure 4. Comparison of adsorbed isopropanol (IPA) mineralization on Mn_xO_y surface using three different regeneration methods. Reprinted from Ref. [50], with permission from Elsevier.

$$O_3 + Mn_xO_y \xrightarrow{296\ K} Mn_xO_{y-}O_2^{ads} + [O] \quad (3)$$

$$CH_3CHOHCH_3{}^{ads} \xrightarrow{[O_3]\ and\ [O]} C_3H_6O^{ads} + Mn_xO_{y-}O_2^{ads} + CH_3CHOHCH_{3(g)} + C_3H_6O_{(g)} \quad (4)$$

$$C_3H_6O^{ads} + Mn_xO_{y-}O_2^{ads} \xrightarrow{[O]} [intermediate\ species] + CO_{2(g)} + CO_{(g)} + CO_3^{-ads} + HCOO^{-ads} \quad (5)$$

$$CH_3CHOHCH_3{}^{ads} \xrightarrow{[O]} [intermediate\ species] + CO_{2(g)} + CO_{(g)} + CO_3^{-ads} + HCOO^{-ads} \quad (6)$$

$$[intermediate\ species] + CO_3^{-ads} + HCOO^{-ads} \xrightarrow{TPD} C_3H_6O_{(g)+}CO_{2(g)} + CO_{(g)} \quad (7)$$

$$CH_3CHOHCH_3{}^{ads} \xrightarrow{NTP} CO_{2(g)} + CO_{(g)} \quad (8)$$

$$CH_3CHOHCH_3{}^{ads} \xrightarrow{NTP} C_3H_6O^{ads} \xrightarrow{NTP} CO_{2(g)} + CO_{(g)} \quad (9)$$

$$CH_3CHOHCH_3{}^{ads} \xrightarrow{NTP} [intermediate\ species] \xrightarrow{NTP} CO_{2(g)} + CO_{(g)} \quad (10)$$

A new hybrid approach consisting of a concentration technique, followed by surface discharge plasma treatment is reported by Yamamoto *et al.* [57]. The process of alternate adsorption and desorption was carried out in the concentration technique where a molecular sieve was used as adsorbent and thermal heat was used to desorb toluene. The purpose of using this concentration technique is to convert low concentrated high flow rate flue gases into a low flow rate gases with high concentrations of VOCs. As a result, the size, energy consumption and operating costs of such cyclic systems are greatly reduced. Experiments revealed that more than 90% toluene decomposition efficiency was achieved by using two surface discharge units at 25 W while the energy efficiency was 34.2 g/kWh. On the other hand, the energy efficiency for continuous plasma treatment was only 1.97 g/kWh. These findings show that the consecutive process of adsorption, desorption and plasma decomposition requires 17 times less energy than the continuous plasma treatment.

The studies mentioned above mainly focus on the adsorbed VOCs oxidation performance by plasma without gas circulation. Few studies have, however, been conducted on plasma-catalytic oxidation performance with a gas circulation. For instance, investigation of plasma-catalytic oxidation of adsorbed toluene using gas circulation with MnO_x and AgO_x catalyst have been reported by Dang *et al.* [58]. Experiments revealed that when MnO_x/ɣ-Al_2O_3 is used, continuous cycle mode exhibits better CO_x yield (11% higher) than intermittent cycle mode due to the enhanced utilization of reactive species by gas circulation. It is also observed that CO_2 selectivity of MnO_x/ɣ-Al_2O_3 and AgO_x/ɣ-Al_2O_3 catalysts were both close to 100% after a 60 min oxygen plasma treatment.

A pilot-scale test of a toluene oxidation system was developed using an adsorbent (zeolite pellets) and a NTP (surface discharge) with gas circulation by Kuroki *et al.* [59]. When 1 mL of toluene was oxidized for 90 min, the conversion ratio of toluene to CO_x was 88% wherein 94% CO_2 selectivity was achieved. During 6 mL toluene oxidation for 150 min, these values were decreased to 44% and 89%, respectively. However, the authors reported that the conversion rate of toluene to CO_x and the energy efficiency of the toluene to CO_x conversion were increased with the amount of adsorbed toluene. By the same research group, a xylene decomposition system was also investigated using different NTP

plasma sources (60-Hz neon transformer and inverter-type neon transformer) with gas circulation [60]. Inverter-type neon transformer showed better performance (higher conversion ratio of xylene to CO_x and higher energy efficiency) than the 60-Hz neon transformer. However, unstable operation and large amounts of NO_x production makes the inverter-type neon transformer less suitable. A conversion ratio of adsorbed xylene to CO_x of 43% was reached at 60 min and 90% CO_2 selectivity was achieved with the 60-Hz neon transformer.

Another cyclic operation of adsorption and DBD treatment was demonstrated by Yamagata *et al.* for the abatement of diluted toluene (10–120 ppm) from air [52,61]. Experiments were carried out with and without gas circulation. For the latter case, enhanced decomposition efficiency was obtained with insertion of the honeycomb zeolites in the DBD reactor compared to the plasma alone system. It is suggested that an increase of the residence time due to adsorption of toluene on the zeolites honeycomb sheet is responsible for the enhanced performance. Under gas circulation with 150 L/min flow rate, the decomposition ratio was 70% to 93% while the energy efficiency was 19 to 8.4 g/kWh. Successful regeneration of zeolites honeycomb sheet was also reported with this sequential treatment.

3. Critical Process Parameters for VOC Adsorption

The most important parameters for the selection of an appropriate adsorbent are capacity, selectivity, regenerability and cost. Adsorption capacity is the most prominent characteristic of an adsorbent and is defined as the amount of adsorbate accumulated on the adsorbent surface, per unit mass or volume of the adsorbent. It is evident that better adsorption capacity assists to reduce the overall energy consumption of the process [39]. In most literature, adsorption capacity is expressed by means of an adsorption isotherm, which plots the loading/capacity as a function of concentration at constant temperature. Adsorption isotherms can provide valuable information about the surface chemistry, the fundamentals involved in the adsorption process and estimation of the surface area, pore volume and pore size. Common adsorbents are inorganic materials such as alumina (Al_2O_3), silica gel, zeolites and organic materials such as activated carbon (AC) and polymers. In the following sections, the parameters that affect the adsorption process will be discussed in more detail.

3.1. Physical Properties of Sorbent/Catalyst

The adsorption capacity greatly depends on the surface roughness quantified by the specific surface area (m^2/g). By increasing the specific surface area, the adsorption capacity will be improved. Activated carbon, alumina and silica gel are considered as excellent adsorbents owing to their highly porous structures and large surface areas. Surface area of a powdered adsorbent depends upon its particle size: the particle size is inversely proportional to the specific surface area. Thus, finely divided metals such as nickel and platinum provide a large surface area and are ideal adsorbents. VOC adsorption capacity also depends on material pore volume, pore size, pore size distribution and diffusion rate, cation exchange capacity, pH and surface functional groups [62–64].

The mechanism of adsorption is dependent upon the size of the VOC molecules in comparison with the pore diameter of the adsorbent due to the energetic interactions between the chosen adsorbate and the pores [65]. It has been shown that the adsorption energy depends on the size of pores in adsorbents [66]. The enlargement of pore size reduces the overlapping potential for adsorbate between

pore walls leading to lower adsorption energy [67]. Huang *et al.* have demonstrated that the capacity for VOCs adsorption on ACs is controlled by characteristics adsorption energy, which is inversely proportional to the local pore size [68]. VOC molecules tend to adsorb most strongly in areas where the pore diameter of the adsorbent is close to the molecular diameter of the VOCs. For instance, in a silicalite ZSM-5 with narrow pores of 5.5 Å diameter, the methyl ethyl ketone (MEK) molecules with a kinetic diameter of 5.2 Å interact strongly with the channel walls, whereas this interaction is much smaller in large pores of aluminosilicates such as de-aluminated faujasite Y (Fau-Y-7.4 Å) [69]. The effect of the porosity and the surface chemistry of ACs on the adsorption capacity of low concentrated VOCs (benzene and toluene) has been investigated by Lillo-Rodenas *et al.* [70,71]. Experiments revealed that in order to maximize the adsorption capacities of diluted VOCs, an AC surface discharge combined with a large volume of narrow micropores (*i.e.*, pore size below 0.7 nm) and reduced surface oxygen groups are desired.

3.2. Nature of VOCs

The amount of adsorbate depends on the nature of VOCs. In general, the higher its critical temperature or van der Waals' force of attraction, the more readily it will adsorb [64]. This is only valid for physisorption, since in this case the adsorbate physically adsorbs on the surface of adsorbents as a result of van der Waals interactions. Generally three different types of interaction exist among molecules, which contribute to the van der Waal's forces. These are instantaneous dipole-induced dipole interactions, dipole-induced dipole interactions between polar and neutral nonpolar molecules and dipole-dipole interactions between polar molecules. Furthermore, the strength of van der Waals' forces typically depends on three properties, *i.e.*, molecule size, surface area and polarity. For instance, the surface of AC is basically nonpolar and will weakly interact with polar VOC molecules such as acetone [68]. Since chemisorption involves a chemical reaction between the adsorbent and the adsorbate, new types of electronic bonds (ionic or covalent) are created. Due to specificity, the nature of chemisorption depends on the chemical nature of the VOC and the surface morphology.

VOCs vapor pressure or boiling point is generally used to quantify the intermolecular interactions instead of their polarity. Polar compounds have higher boiling points or lower vapor pressures than non-polar compounds. VOCs, which have a high molecular weight and high boiling point can be effectively adsorbed on AC [72]. At higher boiling points, liquefaction and condensation occur more readily leading to increased adsorption capacity [67,68]. The influence of VOC molecular size and shape on adsorption has also been investigated by Yang *et al.* [73]. Experiments revealed that the VOC adsorption capacity on Metal-organic frameworks MIL-101 ($Cr_3F(H_2O)_2OE(O_2C)–C_6H_4–(CO_2)_3 \cdot nH_2O$; n is ~25) decreased with an increase in VOC molecular cross sectional area since large VOC molecules cannot penetrate through the smaller size of MIL-101 cylindrical micropores. Adsorption of VOCs on MIL-101 also showed shape selectivity towards VOCs molecules: The adsorption capacity of p-xylene was higher than that of *m*-xylene and *o*-xylene even though they have almost equal molecule cross-sectional areas (Figure 5).

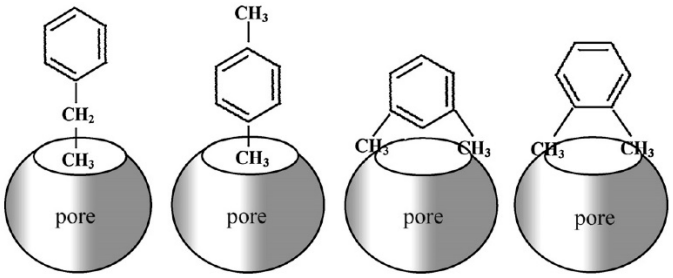

Figure 5. Scheme of ethyl benzene, *p*-xylene, *o*-xylene and *m*-xylene entering into MIL-101 pores. Reprinted from Ref. [73], with permission from Elsevier.

It has also been observed that the VOC concentration can have a positive influence on the adsorption capacity of a material [22,72] and that other chemical properties of VOCs such as oxidation state can also influence adsorption.

3.3. Relative Humidity

The effect of humidity is of great interest for practical applications in industry as well as non-industrial buildings since moisture is always present in to some degree in ambient air. Regarding VOC adsorption, RH might change the chemical state of the sorbent surface or change the adsorption modes and adsorbed amount of VOC on sorbent. It seems that the effect of RH is determined by the VOC-sorbent combination. VOC adsorption can be enhanced, suppressed or remain neutral when air humidity changes, depending on the hydrophobicity of the sorbent and specific VOC properties like e.g., solubility. Kuroki *et al.* have mentioned that the influence of RH is negligible in a toluene adsorption process since hydrophobic zeolite honeycomb is used [74]. Similarly, Zhao *et al.* have investigated HCHO breakthrough capacity over AgCu/HZ catalyst in air with varying *R*H (dry gas and *R*H = 20%, 50%, 80% and 93%) [39]. HCHO breakthrough capacity slightly decreases in humid condition compared to dry gas. However, breakthrough capacity remains almost constant when RH changes from 20% to 93% due to the hydrophobic property of high-silica zeolite. Sivachandiran *et al.* have precisely investigated the impact of RH on IPA adsorption over TiO_2 [35]. The influence of air RH on reversibly and irreversibly adsorbed IPA on TiO_2 is shown in Figure 6. The amount of both reversibly as well as irreversibly adsorbed IPA continuously decreases with increasing RH. The result suggests possible competitive adsorption between water vapor and IPA molecules. Even at the lowest moisture (10% RH) content, the partial pressure of H_2O is quite high compared to IPA. Hence, H_2O adsorption is more favorable in this competitive process. Interestingly, the amount of irreversibly adsorbed IPA increases from 84% to 94% when the water content changes from 35% to 65%. It is expected that water forms a multilayer above 35% RH. Due to high water solubility, part of irreversibly adsorbed IPA will dissolve rather than to directly interact with TiO_2 surface at highest RH.

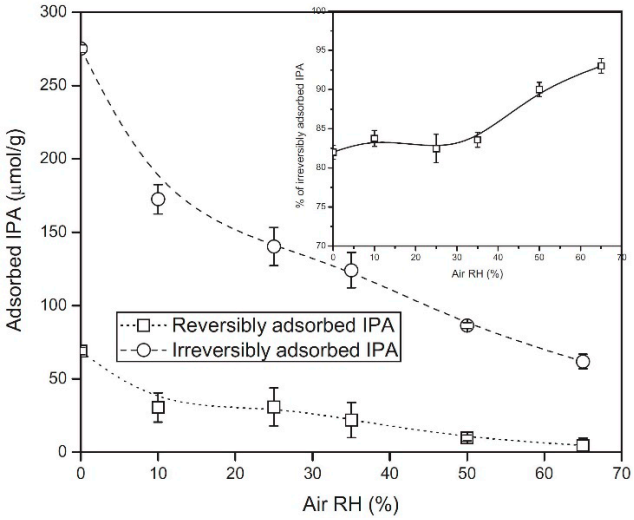

Figure 6. Influence of air relative humidity (RH) on IPA reversible and irreversible adsorbed fractions on TiO_2 at ambient condition. Reprinted from Ref. [35], with permission from Elsevier.

3.4. Temperature

Adsorption process spontaneously occurs when the change in free energy, ΔG, of the system decreases. The entropy change, ΔS, in adsorption process is negative since the adsorbed gas is less mobile than its gaseous state [75]. Therefore, the heat of adsorption, ΔH, must always be negative since $\Delta G = \Delta H - T\Delta S$. Thus, adsorption is always exothermic. The heat of adsorption also defines the extent of the interactions between adsorbate molecules and adsorbent lattice atoms. Physisorption is predominant at lower temperatures due to weak Van Der Waals' forces interactions. Since chemical reaction probability increases with temperature, chemisorption is favored at high temperatures. In most circumstances, the amount of adsorption decreases however with increasing temperature. For instance, Song *et al.* demonstrated that the breakthrough time for the adsorption process was significantly reduced at elevated temperatures compared to room temperature indicating lower adsorption capacity [32]. Brodu *et al.* have reported the influence of temperature on MEK adsorption capacity of two aluminosilicates (Fau-Y, ZSM-5) [69]. The quantity of adsorbed MEK on both Fau-Y and ZSM-5 decreased with increasing temperature. On Fau-Y, the adsorption rate of MEK was 87% at 298 K and 51% at 333 K, respectively. This clearly indicates a higher loss of adsorption capacity with rising temperature. However, some researchers have observed an enhanced adsorption capacity of AC in the high temperature range [76]. In this experiment, adsorption of four VOCs including carbon tetrachloride (CCl_4), chloroform ($CHCl_3$), benzene and methylene chloride (CH_2Cl_2) on AC at different temperatures was carried out. For a given VOC concentration, the adsorbed amount of VOC decreased with increasing temperature except for benzene. This abnormal behavior of benzene is attributed to the activated entry effect, which is responsible for the temperature-dependent nature of equilibrium adsorption [77]. At higher temperature, the diffusion of benzene molecules is facilitated into the narrow micropore channels. This promotes the rate of entry into the micropores leading to enhanced adsorption capacity.

4. Critical Process Parameters for Regeneration

To ensure an economically feasible process with uniform performance of sequential treatment, the regenerability of an adsorbent is considered as the most important parameter. The conventional and most popular regeneration techniques are thermal swing, pressure swing and chemical regeneration (displacement, elution, supercritical extraction) or a combination of those. As this review article is related to plasma regeneration processes, only the influence of process parameters on the regeneration by plasma will be discussed in the following sections.

4.1. Flow Rate

The effect of gas flow rate on the regeneration efficiency has been studied by several groups. When gas flow rate increases the residence time/space time of the gas stream is lowered. This will decrease the plasma exposure time during the regeneration stage leading to a suppression of the decomposition efficiency. Saulich *et al.* have investigated the influence of the N_2 flow rate in a DBD packed with MP 5 on the decomposition of adsorbed HCHO [48]. From Figure 7, it is apparent that with higher N_2 flow rate, the total amount of decomposed HCHO molecules increases and the formation of CO_2 is greatly favored.

However, Kuroki *et al.* have reported opposite phenomena during the adsorption of toluene with a DBD packed with a hydrophobic zeolite honeycomb [74]. According to the authors, at a low gas flow rate, re-adsorption may occur inside the adsorbent during the plasma desorption process, resulting in a lower decomposition efficiency. Therefore, the optimum gas flow rate should be determined.

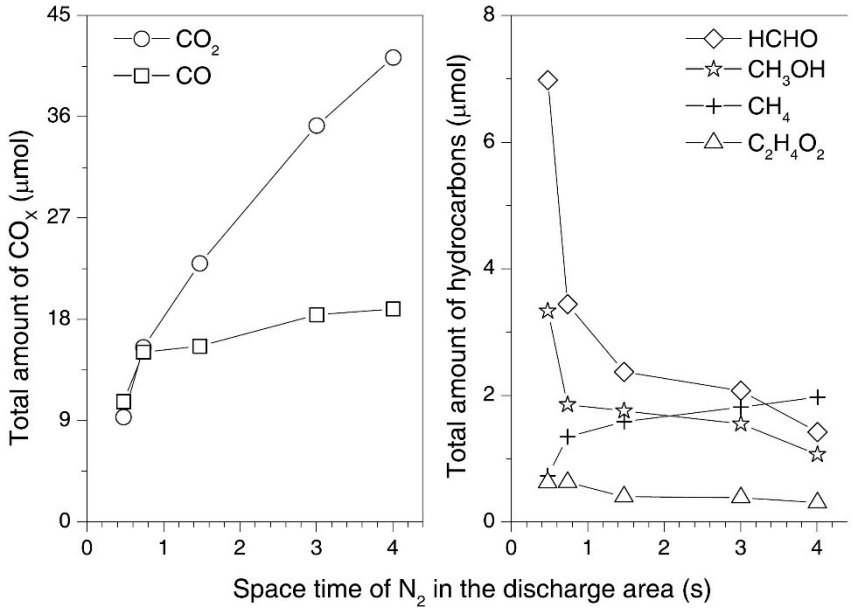

Figure 7. Influence of flow rate on the decomposition of formaldehyde (HCHO) adsorbed on MP 5 (adsorption: 176 mL/min flow rate of polluted N_2 with 99 ppm of HCHO, adsorption time t_1 = 250 min, total amount of adsorbed HCHO: 155 µmol; discharge carrier gas N_2, discharge power P = 2.2 W). Reprinted from Ref. [48], with permission from Elsevier.

4.2. Temperature

Temperature has an influence on the electrical properties of a NTP discharge. With varying temperature, the gas density varies, leading to a change in reduced electric field strength (E/N). Generally, it is known that the kinetic reaction rate of O radicals with VOCs is an increasing function of temperature due to the endothermic reaction behavior. However, the effect of temperature on the production of reactive species such as O radicals still needs detailed studies. Nevertheless, the beneficial influence of temperature on the regeneration process is counteracted by a decrease of the adsorption capacity of the sorbent at higher temperatures. These competitive effects on the plasma-assisted desorption process have been investigated by Song *et al*. who have used a ɣ-Al_2O_3 packed DBD reactor for toluene removal [32]. As expected, the thermal decomposition of NTP produced ozone increases with elevated temperature. The removal rate of adsorbed toluene on ɣ-Al_2O_3 beads was also improved at higher temperatures compared to room temperature. In addition, ɣ-Al_2O_3 was able to reduce some other by-products, such as O_3 and HNO_3.

4.3. Discharge Power

The oxidative ability of NTP treatment for adsorbent regeneration can be improved by increasing input power. Indeed, there is an optimal discharge power at which high oxidation rate and low energy cost can be achieved. The effect of discharge power on the plasma catalytic oxidation of adsorbed benzene over metal supported zeolite (Ag/HZSM-5) catalyst has been studied by Hong-Yu *et al.* [40] (Figure 8a). The optimum DBD operating power is found to be 4.7 W at which almost 100% of adsorbed benzene is oxidized to CO_2. The energy cost at this optimum power was as low as 3.7×10^{-3} kWh/m³.

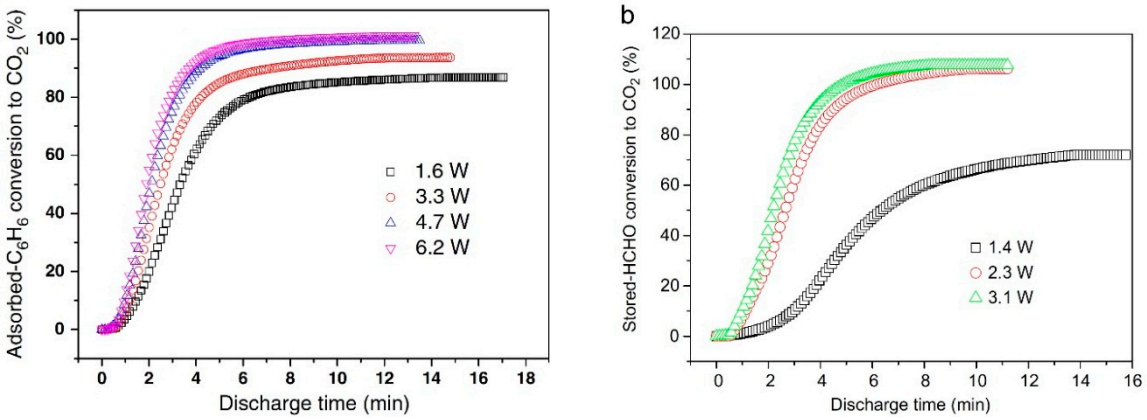

Figure 8. (**a**) Adsorbed-benzene conversion to CO_2 over Ag/HZSM-5 catalysts (**b**) stored-HCHO conversion to CO_2 over AgCu/HZ catalysts as a function of discharge time at various discharge powers. Reprinted from Ref. [39,40], with permission from Elsevier.

Zhao *et al.* have also investigated the effect of discharge power on the plasma catalytic oxidation of stored HCHO on AgCu/HZ catalyst [39]. The conversion of HCHO to CO_2 dramatically increases

(Figure 8b) reaching almost 100% after 5 min of operation at 2.3 W. Further increase of the discharge power did not significantly improve the HCHO conversion.

The influence of discharge power on toluene decomposition has also been studied by Mok *et al.* [46] where complete toluene decomposition towards CO and CO_2 was reported instead of quantifying the CO_x selectivity. With increasing discharge power, the concentration of CO and CO_2 further increased indicating faster oxidation of adsorbed toluene.

Sivachandrian *et al.* have precisely investigated the effect of discharge power on the regeneration of adsorbed acetone on TiO_2 surface [47]. They applied a double DBD with TiO_2 coated glass beads. Although the oxidation rate of acetone is improved with increasing input power, the removal efficiency remains constant around 25%. To achieve both sufficient surface regeneration and high mineralization, 0.33 W is considered as an optimum input power. The authors confirmed that even though the regeneration efficiency was limited during NTP treatment, operation at moderate discharge power modified the nature of organic adsorbed species, which facilitated mineralization during successive thermal treatments (Figure 9). Modification of adsorbed acetone *i.e.*, mesityl oxides into formic acid is only possible above 0.13 W. Hence, acetone desorption is decreased while CO and CO_2 formation are promoted by increasing input power during successive thermal treatment. Any further increase of input power above 0.33 W is useless regarding conversion of mesityl oxide into formic acid.

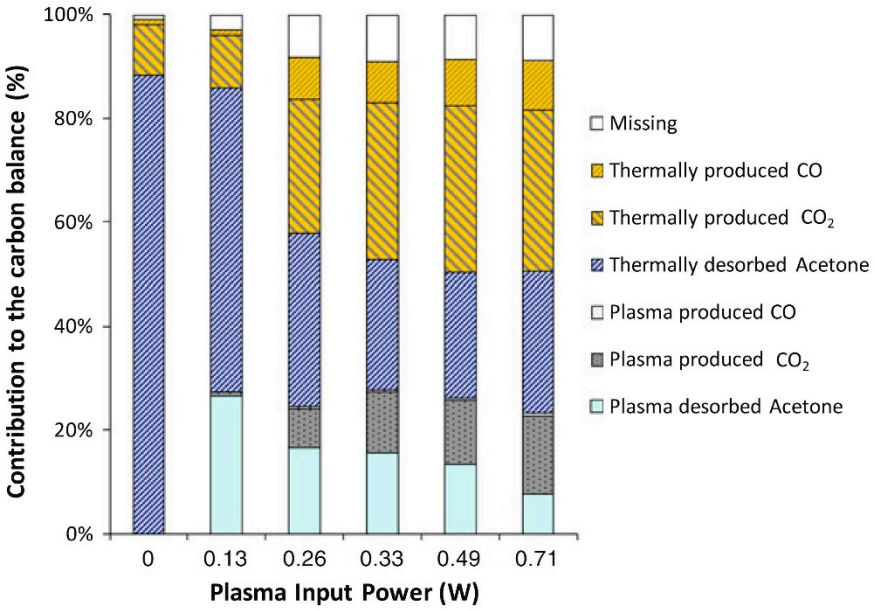

Figure 9. Contributions of CO, CO_2 and acetone to the carbon balance, calculated after successive plasma treatment and thermal treatment. Data are displayed for various plasma input powers. Reprinted from Ref. [47], with permission from Elsevier.

4.4. Relative Humidity

During real-time operation, humidity is permanently present in air, which will impact both the adsorption mechanism and regeneration process unless hydrophobic sorbents are used. Fan *et al.* have studied the removal of low concentrated benzene stored on 0.8% Ag/HZSM-5 catalyst under various humidity conditions (dry air and *R*H = 20%, 50% and 80%) [42]. Figure 10 shows that the oxidation

rate slightly decreases up to 50% RH compared to dry air. However, CO_2 selectivity and carbon balance reached almost 100% in all cases. The plausible explanation of this weak effect of humidity on oxidation rate is the hydrophobic property of high-silica zeolite. Therefore, this result should be limited only to hydrophobic surfaces; moreover, no RH was introduced during the plasma-assisted regeneration process. The presence of humidity can influence the electrical and physical properties of the discharge as well as the plasma chemistry. For instance, the RH can affect the input power and change the nature and amounts of reactive plasma species, which will have an influence on the VOC oxidation pathway.

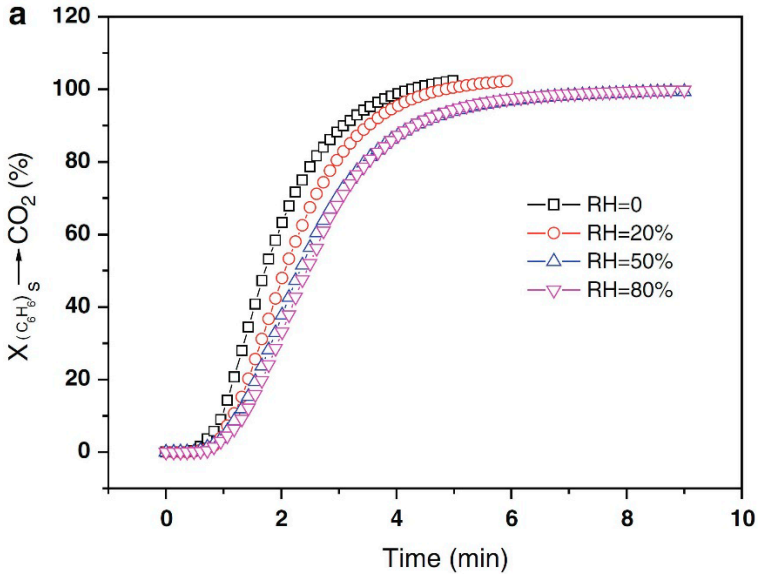

Figure 10. Effect of relative humidity (RH) on plasma catalytic oxidation of stored benzene over 0.8 wt.% Ag/HZ catalysts to CO_2 (storage stage: 4.7 ppm benzene, 0%–80% RH (25 °C), 600 mL/min flow rate of simulated air, t_1 = 1 h; discharge stage with 60 mL/min O_2, P = 4.7 W. Reprinted from Ref. [42], with permission from Elsevier.

To assess the impact of RH on both the adsorption modes and the surface plasma regeneration efficiency, Sivachandiran *et al.* have investigated the removal of IPA with a packed bed reactor coated with TiO_2 under various RH conditions [35]. Increased RH favored IPA mineralization and diminished acetone formation. With increasing RH from 0% to 65%, the carbon balance enhanced from 36% to 91%, clearly proving that moisture has a positive influence on the plasma surface regeneration efficiency. The authors suggest that dissociative electron impact with H_2O produces OH radicals, which are chemisorbed on TiO_2 leading to re-hydroxylation of the pre-treated TiO_2 surface. Eventually, adsorbed IPA will be replaced by hydroxyl groups and desorb. Generally, the oxidation power of OH radicals is much stronger than other oxidants such as oxygen atoms and peroxyl radicals. Increased RH favors production of OH radicals and the subsequent oxidation of VOCs leading to high mineralization rate. In comparison to dry-air experiments, almost 80% acetone production was reduced in the presence of only 10% air RH. Low surface coverage of TiO_2 by H_2O molecules allows the adsorption of the deprotonated CH_3–CHO^*–CH_3 species onto the TiO_2 surface [35]. Indeed, in case of humid air, the most common oxidation pathway for VOC removal with NTP is the H-atom abstraction by

OH radicals. [78]. Since large amounts of OH radicals are produced by the discharge in the surface vicinity, it improves the dehydrogenation of IPA hydroxyl groups leading to the formation of acetone [35]. However, above 25% RH, formation of a water multilayer onto the TiO_2 surface impeded the dissociative adsorption of IPA onto the TiO_2 surface obstructing acetone formation.

4.5. O_2 Content/O_2 Partial Pressure

Similar to air RH, the discharge properties and VOC abatement process are sensitive to oxygen content. The presence of oxygen in the discharge generally increases the amount of O radicals leading to a high removal efficiency. However, owing to its electronegative character, oxygen limits the electron density and also reduces the formation of other reactive species e.g., N_2 and N_2*, which are beneficial for VOC abatement [79–81]. Saulich *et al.* have used a mineral adsorbent packed DBD reactor to see the effect of O_2 on the plasma decomposition process of adsorbed HCHO [48]. Addition of 10% O_2 to N_2 increased both the formaldehyde decomposition efficiency and the mineralization rate compared to pure N_2. Kim *et al*. have demonstrated the effect of oxygen content on benzene decomposition using a plasma-catalyst reactor (5% Cu/MOR) [82]. Figure 11 clearly shows that when the plasma is turned on after the adsorption mode, benzene concentration decreases and CO and CO_2 formation simultaneously increases with increasing O_2 percentage. Several catalysts (TiO_2, ɣ-Al_2O_3, zeolites) loaded with nanoparticles of active metals (Ag, Cu, Zr) or noble metals (Pt, Pd) have also been investigated under various oxygen partial pressures for toluene and benzene abatement [29]. The increase of O_2 content enhanced both the decomposition efficiency (~30%–100%) and the CO_2 selectivity regardless of the catalyst type [29]. Operating the regeneration mode at high O_2 content leads to complete oxidation of VOCs without CO, aerosol and N_xO_y formation and complete decomposition of VOCs to CO_2 is achieved with the CSD system under O_2 plasma in most literature so far.

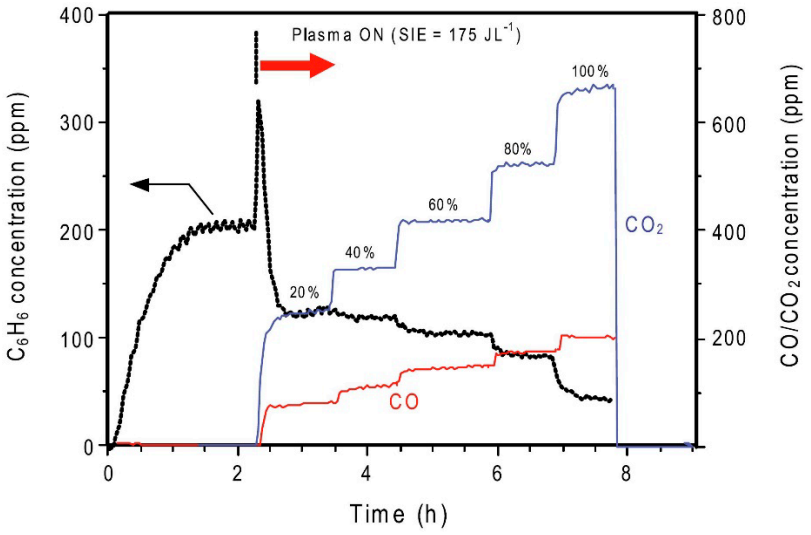

Figure 11. Effect of oxygen content on the volatile organic compounds (VOC) decomposition using a plasma-catalyst reactor (5 wt.% Cu/MOR). Applied voltage and frequency were kept constant at 16 kV and 300 Hz, respectively. Temperature was 100 °C. Space velocity was 33,000/h. Reprinted from Ref. [82], with permission from Elsevier.

4.6 Number of Cycles

Potential irreversible ageing of adsorbent may occur during the regeneration process, which governs the life of an adsorbent. After multiple regeneration cycles, the adsorbent may not fully recover its initial properties, such as the specific surface area or adsorption capacity [83]. Adsorption capacity may decrease due to surface modification by particle agglomerations or polymerization on the catalyst surface, which results in blocking active sites during the regeneration step. Keeping this in mind, researchers should also inspect the effect after the repeatability test of this sequential treatment. For instance, Kuroki *et al*. performed a repeatability test of adsorption and plasma desorption and reported that toluene was almost completely adsorbed over honeycomb zeolites in each adsorption process [84]. Having 75% regeneration efficiency, both desorption and regeneration efficiencies do not deteriorate for 10 repetitions of the adsorption/desorption processes (Figure 12). Similarly, seven repetitive adsorption-discharge cycles were performed for HCHO abatement from mineral adsorbent by Saulich *et al*. [48]. Adsorption capacity and regeneration efficiency were found to be more or less the same in each cycle [48]. The stability of AgCu/HZ catalyst during five consecutive storage-discharge cycles was also examined by D. Zhao *et al.* [39]. HCHO storage capacity was almost constant, and CO_2 selectivity and carbon mass balance were maintained at ~100%.

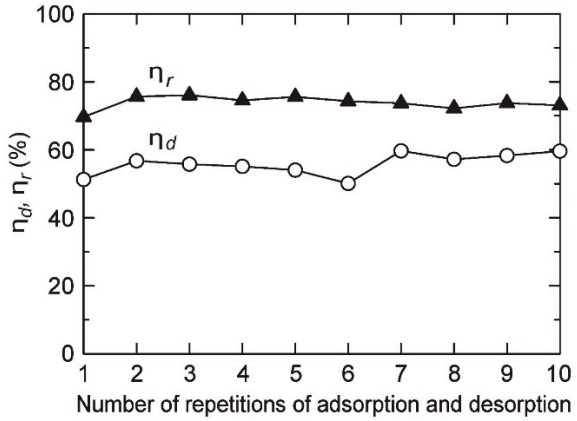

Figure 12. Desorption and regeneration efficiencies denoted by η_d and η_r, respectively, as a function of repetitive operation. Reprinted from Ref. [84], with permission from Elsevier.

5. Conclusions

From the review above, it can be concluded that sequential treatment has attracted growing interest among researchers and has proven to be an effective method for VOC abatement as well as for regeneration of saturated adsorbents. However, choosing an appropriate catalyst to achieve the best performance is still a challenge since it has to combine high adsorption capacity with high catalytic activity for oxidation of adsorbed VOCs. For instance, hard-to-adsorb VOC molecules are not appropriate for adsorption processes [61]. The key factor for the abatement of this kind of compounds is either to choose appropriate catalyst materials with a large adsorption capacity or to remove them through continuous treatment.

Although the review of experimental results of cyclic VOC adsorption and plasma-assisted regeneration shows substantial progress, many questions still remain unanswered regarding the impact

of process parameters and VOCs degradation mechanisms. In this regard, direct *in-situ* surface monitoring of the catalyst/adsorbent will be crucial to elucidate these important issues. Furthermore, modeling and simulation studies would also contribute to the understanding of the various underlying plasma-catalytic effects.

The research on sequential plasma-catalysis coupling for VOC abatement has mostly been performed on the laboratory scale. Up to now, only a few studies on pilot scales with gas circulation have been reported [59]. To achieve an economically feasible VOC removal process without gas circulation, cyclic operation of VOC adsorption and catalyst regeneration has been proposed by researchers. In this regard, future work should focus on the feasibility and optimization of the duration of the sequential intervals. Finally, to realize industrial implementation of this energy effective method for VOC abatement scalability studies will also need to be carried out in the near future.

Author Contributions

Sharmin Sultana wrote the first draft of the review which was then refined by the comments and suggestions of all other authors.

Conflicts of Interest

The authors declare no conflict of interest.

References

1. Pal, R.; Kim, K.-H.; Hong, Y.-J.; Jeon, E.-C. The Pollution Status of Atmospheric Carbonyls in a Highly Industrialized Area. *J. Hazard. Mater.* **2008**, *153*, 1122–1135.
2. Sarigiannis, D.A.; Karakitsios, S.P.; Gotti, A.; Liakos, I.L.; Katsoyiannis, A. Exposure to Major Volatile Organic Compounds and Carbonyls in European Indoor Environments and Associated Health Risk. *Environ. Int.* **2011**, *37*, 743–765.
3. Atkinson, R. Atmospheric Chemistry of VOCs and NO_x. *Atmos. Environ.* **2000**, *34*, 2063–2101.
4. Vineis, P.; Forastiere, F.; Hoek, G.; Lipsett, M. Outdoor Air Pollution and Lung Cancer: Recent Epidemiologic Evidence. *Int. J. Cancer* **2004**, *111*, 647–652.
5. Tollefsen, P.; Rypdal, K.; Torvanger, A.; Rive, N. Air Pollution Policies in Europe: Efficiency Gains From Integrating Climate Effects with Damage Costs to Health and Crops. *Environ. Sci. Policy* **2009**, *12*, 870–881.
6. Yamamoto, T.; Ramaanathan, K.; Lawless, P.A.; Ensor, D.S.; Newsome, J.R.; Plaks, N.; Ramsey, G.H. Control of Volatile Organic Compounds by an AC Energized Eerroelectric Pellet Reactor and a Pulsed Corona Reactor. *IEEE Trans. Ind. Appl.* **1992**, *28*, 528–534.
7. Nunez, C.M.; Ramsey, G.H.; Ponder, W.H.; Abbott, J.H.; Hamel, L.E.; Kariher, P.H. Corona Destruction: An Innovative Control Technology for VOCs and Air Toxics. *Air Waste* **1993**, *43*, 242–247.
8. Sudnick, J.J.; Corwin, D.L. VOC Control Techniques. *Hazard. Waste Hazard.* **1994**, *11*, 129–143.
9. Kim, H.H.; Ogata, A.; Futamura, S. Complete Oxidation of Volatile Organic Compounds (VOCs) Using Plasma-Diven Catalysis and Oxygen Plasma. *Int. J. Plas. Environ. Sci. Tech.* **2007**, 4–8.

10. Keller, R.A.; Dyer, J.A. Abating Halogenated VOCs. *Chem. Eng.* **1998**, *105*, 100–105.
11. Dyer, J.A.; Mulholland, K. Toxic Air Emissions What is the Full Cost to Your Business? *Chem. Eng.* **1994**, *101*, 4–8.
12. Urashima, K.; Chang, J.S. Removal of Volatile Organic Compounds from Air Streams and Industrial Flue Gases by Non-thermal Plasma Technology. *IEEE Trans. Dielectr. Electr. Insul.* **2000**, *7*, 602–614.
13. Chang, J.S. Next Generation Integrated Electrostatic Gas Cleaning Systems. *J. Electrostat.* **2003**, *57*, 273–291.
14. Dan, Y.; Gao, D.S.; Yu, G.; Shen, X.L.; Gu, F. Investigation of the Treatment of Particulate Matter from Gasoline Engine Exhaust Esing Non-thermal Plasma. *J. Hazard. Mater.* **2005**, *127*, 149–155.
15. Laroussi, M. Low Temperature Plasma-based Ssterilization: Overview and State-of-the-art. *Plasma Process. Polym.* **2005**, *2*, 391–400.
16. Chang, C.L.; Lin, T.S. Decomposition of Toluene and Acetone in Packed Dielectric Barrier Discharge Reactors. *Plasma Chem. Plasma Process.* **2005**, *25*, 227–243.
17. Lee, H.M.; Chang, M.B. Gas-phase Removal of Acetaldehyde Via Packed-bed Dielectric Barrier Discharge Reactor. *Plasma Chem. Plasma Process.* **2001**, *21*, 329–343.
18. Okubo, M.; Yamamoto, T.; Kuroki, T.; Fukumoto, H. Electric Air Cleaner Composed of Nonthermal Plasma Reactor and Electrostatic Precipitator. *IEEE Trans. Ind. Appl.* **2001**, *37*, 1505–1511.
19. Vandenbroucke, A.M.; Mora, M.; Jimenez-Sanchidrian, C.; Romero-Salguero, F.J.; de Geyter, N.; Leys, C.; Morent, R. TCE Abatement with a Plasma-catalytic Combined System Using MnO_2 as Catalyst. *Appl. Catal. B* **2014**, *156*, 94–100.
20. Nguyen Dinh, M.T.; Giraudon, J.M.; Lamonier, J.F.; Vandenbroucke, A.; de Geyter, N.; Leys, C.; Morent, R. Plasma-catalysis of Low TCE Concentration in air Using $LaMnO_3{}^{+}\delta$ as Catalyst. *Appl. Catal. B* **2014**, *147*, 904–911.
21. Assadi, A.A.; Palau, J.; Bouzaza, A.; Penya-Roja, J.; Martinez-Soriac, V.; Wolbert, D. Abatement of 3-methylbutanal and Trimethylamine with Combined Plasma and Photocatalysis in a Continuous Planar Reactor. *J. Photoch. Photobiol. A* **2014**, *282*, 1–8.
22. Ohshima, T.; Kondo, T.; Kitajima, N.; Sato, M. Adsorption and Plasma Decomposition of Gaseous Acetaldehyde on Fibrous Activated Carbon. *IEEE Trans. Ind. Appl.* **2010**, *46*, 23–28.
23. Kim, H.H.; Ogata, A.; Futamura, S. Effect of Different Catalysts on the Decomposition of VOCs Using Flow-type Plasma-driven Catalysis. *IEEE Trans. Plasma Sci.* **2006**, *34*, 984–995.
24. Vandenbroucke, A.M.; Minh Tuan Nguyen, D.; Giraudon, J.-M.; Morent, R.; De Geyter, N.; Lamonier, J.-F.; Leys, C. Qualitative By-product Identification of Plasma-assisted TCE Abatement by Mass Spectrometry and Fourier-transform Infrared Spectroscopy. *Plasma Chem. Plasma Process.* **2011**, *31*, 707–718.
25. Van Durme, J.; Dewulf, J.; Leys, C.; Van Langenhove, H. Combining Non-thermal Plasma with Heterogeneous Catalysis in Waste Gas Treatment: A Review. *Appl. Catal. B* **2008**, *78*, 324–333.
26. Roland, U.; Holzer, F.; Kopinke, E.D. Combination of Non-thermal Plasma and Heterogeneous Catalysis for Oxidation of Volatile Organic Compounds Part 2. Ozone Decomposition and Deactivation of γ-Al_2O_3. *Appl. Catal. B* **2005**, *58*, 217–226.

27. Subrahmanyam, C. Catalytic Non-thermal Plasma Reactor for Total Oxidation of Volatile Organic Compounds. *Indian J. Chem. A* **2009**, *48*, 1062–1068.
28. Zhu, T.; Li, J.; Liang, W.J.; Jin, Y.Q. Synergistic Effect of Catalyst for Oxidation Removal of Toluene. *J. Hazard. Mater.* **2009**, *165*, 1258–1260.
29. Kim, H.H.; Ogata, A.; Futamura, S. Oxygen Partial Pressure-dependent Behavior of Various Catalysts for the Total Oxidation of VOCs Using Cycled System of Adsorption and Oxygen Plasma. *Appl. Catal. B* **2008**, *79*, 356–367.
30. Malik, M.A.; Minamitani, Y.; Schoenbach, K.H. Comparison of Catalytic Activity of Aluminum Oxide and Silica Gel for Decomposition of Volatile Organic Compounds (VOCs) in a Plasmacatalytic Reactor. *IEEE Trans. Plasma Sci.* **2005**, *33*, 50–56.
31. Ogata, A.; Yamanouchi, K.; Mizuno, K.; Kushiyama, S.; Yamamoto, T. Oxidation of Dilute Benzene in an Alumina Hybrid Plasma Reactor at Atmospheric Pressure. *Plasma Chem. Plasma Process.* **1999**, *19*, 383–394.
32. Song, Y.H.; Kim, S.J.; Choi, K.I.; Yamamoto, T. Effects of Adsorption and Temperature on a Nonthermal Plasma Process for Removing VOCs. *J. Electrostat.* **2002**, *55*, 189–201.
33. Martin, L.; Ognier, S.; Gasthauer, E.; Cavadias, S.; Dresvin, S.; Amouroux, J. Destruction of Highly Diluted Volatile Organic Components (VOCs) in air by Dielectric Barrier Discharge and Mineral Bed Adsorption. *Energy Fuel.* **2008**, *22*, 576–582.
34. Inoue, K.; Okano, H.; Yamagata, Y.; Muraoka, K.; Teraoka, Y. PerformanceTtests of Newly Developed Adsorption/plasma Combined System for Decomposition of Volatile Organic Compounds Under Continuous Flow Condition. *J. Environ. Sci. China* **2011**, *23*, 139–144.
35. Sivachandiran, L.; Thevenet, F.; Gravejat, P.; Rousseau, A. Isopropanol Saturated TiO_2 Surface Regeneration by Non-thermal Plasma: Influence of Air Relative Humidity. *Chem. Eng. J.* **2013**, *214*, 17–26.
36. Ogata, A.; Ito, D.; Mizuno, K.; Kushiyama, S.; Yamamoto, T. Removal of Dilute Benzene Using a Zeolte-hybrid Plasma Reactor. *IEEE Trans. Ind. Appl.* **2001**, *37*, 959–964.
37. Thevenet, F.; Sivachandiran, L.; Guaitella, O.; Barakat, C.; Rousseau, A. Plasma-catalyst Coupling for Volatile Organic Compound Removal and Indoor Air Treatment: A Review. *J. Phys. D* **2014**, *47*, 224011–224024.
38. Sivachandiran, L.; Thevenet, F.; Rousseau, A. Isopropanol Removal Using Mn_xO_y Packed Bed Non-thermal Plasma Reactor: Comparison between Continuous Treatment and Sequential Sorption/regeneration. *Chem. Eng. J.* **2015**, *270*, 327–335.
39. Zhao, D.Z.; Li, X.S.; Shi, C.; Fan, H.Y.; Zhu, A.M. Low-concentration Formaldehyde Removal from Air Using a Cycled Storage–discharge (CSD) Plasma Catalytic Process. *Chem. Eng. Sci.* **2011**, *66*, 3922–3929.
40. Fan, H.Y.; Shi, C.; Li, X.S.; Zhao, D.Z.; Xu, Y. High-efficiency Plasma Catalytic Removal of Dilute Benzene from Air. *J. Phys. D* **2009**, *42*, 225105–225109.
41. Ding, H.X.; Zhu, A.M.; Yang, X.F.; Li, C.H.; Xu, Y. Removal of Formaldehyde from Gas Streams via Packed-bed Dielectric Barrier Discharge Plasmas. *J. Phys. D* **2005**, *38*, 4160–4167.
42. Fan, H.-Y.; Li, X.-S.; Shi, C.; Zhao, D.-Z.; Liu, J.-L.; Liu, Y.-X.; Zhu, A.-M. Plasma Catalytic Oxidation of Stored Benzene in a Cycled Storage-discharge (CSD) Process: Catalysts, Reactors and Operation Conditions. *Plasma Chem. Plasma Process.* **2011**, *31*, 799–810.

43. Wang, W.; Zhu, T.; Fan, X. Removal of Gas Phase Low-concentration Toluene by Intermittent Use of Adsorption and Non-thermal Plasma Regeneration. In Proceedings of 21st International Symposium on Plasma Chemistry (ISPC 21), Queensland, Australia, 4–9 August 2013.
44. Takahashi, A.; Yang, F.H.; Yang, R.T. Aromatics/aliphatics Separation by Adsorption: New Sorbents for Selective Aromatics Adsorption by π-complexation. *Ind. Eng. Chem. Res.* **2000**, *39*, 3856–3867.
45. Qu, Z.; Bu, Y.; Qin, Y.; Wang, Y.; Fu, Q. The Improved Reactivity of Manganese Catalysts by Ag in Catalytic Oxidation of Toluene. *Appl. Catal. B* **2013**, *132*, 353–362.
46. Mok, Y.S.; Kim, D.H. Treatment of Toluene by Using Adsorption and Nonthermal Plasma Oxidation Process. *Curr. Appl. Phys.* **2011**, *11*, S58–S62.
47. Sivachandiran, L.; Thevenet, F.; Rousseau, A. Non-thermal Plasma Assisted Regeneration of Acetone Adsorbed TiO_2 Surface. *Plasma Chem. Plasma Process.* **2013**, *33*, 855–871.
48. Saulich, K.; Mueller, S. Removal of Formaldehyde by Adsorption and Plasma Treatment of Mineral Adsorbent. *J. Phys. D* **2013**, *46*, 045201–045208.
49. Klett, C.; Duten, X.; Tieng, S.; Touchard, S.; Jestin, P.; Hassouni, K.; Vega-González, A. Acetaldehyde Removal Using an Atmospheric Non-thermal Plasma Combined with a Packed Bed: Role of the Adsorption Process. *J. Hazard. Mater.* **2014**, *279*, 356–364.
50. Sivachandiran, L.; Thevenet, F.; Rousseau, A. Regeneration of Isopropyl Alcohol Saturated Mn_xO_y Surface: Comparison of Thermal, Ozonolysis and Non-thermal Plasma Treatments. *Chem. Eng. J.* **2014**, *246*, 184–195.
51. Barakat, C.; Gravejat, P.; Guaitella, O.; Thevenet, F.; Rousseau, A. Oxidation of Isopropanol and Acetone Adsorbed on TIO_2 Under Plasma Generated Ozone Flow: Gas Phase and Adsorbed Species Monitoring. *Appl. Catal. B* **2014**, *147*, 302–313.
52. Yamagata, Y.; Niho, K.; Inoue, K.; Okano, H.; Muraoka, K. Decomposition of Volatile Organic Compounds at Low Concentrations Using Combination of Densification by Zeolite Adsorption and Dielectric Barrier Discharge. *Jpn. J. Appl. Phys.* **2006**, *45*, 8251–8254.
53. Kim, H.H.; Tsubota, S.; Date, M.; Ogata, A.; Futamura, S. Catalyst Regeneration and Activity Enhancement of Au/TiO_2 by Atmospheric Pressure Nonthermal Plasma. *Appl. Catal. A* **2007**, *329*, 93–98.
54. Arsac, F.; Bianchi, D.; Chovelon, J.M.; Ferronato, C.; Herrmann, J.M. Experimental Microkinetic Approach of the Photocatalytic Oxidation of Isopropyl Alcohol on TiO_2. Part 1. Surface Elementary Steps Involving Gaseous and Adsorbed C_3H_xO species. *J. .Phys. Chem. A* **2006**, *110*, 4202–4212.
55. Larson, S.A.; Widegren, J.A.; Falconer, J.L. Transient Studies of 2-propanol Photocatalytic Oxidation on Titania. *J. Catal.* **1995**, *157*, 611–625.
56. Xu, W.Z.; Raftery, D.; Francisco, J.S. Effect of Irradiation Sources and Oxygen Concentration on the Photocatalytic Oxidation of 2-propanol and Acetone Studied by in situ FTIR. *J. Phys. Chem. B* **2003**, *107*, 4537–4544.
57. Yamamoto, T.; Asada, S.; Iida, T.; Ehara, Y. Novel NO_x and VOC Treatment Using Concentration and Plasma Decomposition. *IEEE Trans. Ind. Appl.* **2011**, *47*, 2235–2240.
58. Dang, X.; Huang, J.; Cao, L.; Zhou, Y. Plasma-catalytic Oxidation of Adsorbed Toluene with Gas Circulation. *Catal. Commun.* **2013**, *40*, 116–119.

59. Kuroki, T.; Hirai, K.; Matsuoka, S.; Kim, J.Y.; Okubo, M. Oxidation System of Adsorbed VOCs on Adsorbent Using Nonthermal Plasma Flow. *IEEE Trans. Ind. Appl.* **2011**, *47*, 1916–1921.
60. Kuroki, T.; Hirai, K.; Kawabata, R.; Okubo, M.; Yamamoto, T. Decomposition of Adsorbed Xylene on Adsorbents Using Nonthermal Plasma with Gas Circulation. *IEEE Trans. Ind. Appl.* **2010**, *46*, 672–679.
61. Inoue, K.; Furuki, K.; Okano, H.; Yamagata, Y.; Muraoka, K. A New Decomposition System for Volatile Organic Compounds Using Combinations of Dielectric Barrier Discharges with Zeolite Honeycomb Sheets. *Electron. Eng. Jpn.* **2009**, *168*, 1–10.
62. Das, D.; Gaur, V.; Verma, N. Removal of Volatile Organic Compound by Activated Carbon Fiber. *Carbon* **2004**, *42*, 2949–2962.
63. Kim, K.-J.; Ahn, H.-G. The Effect of Pore Structure of Zeolite on the Adsorption of VOCs and their Desorption Properties by Microwave Heating. *Microporous Mesoporous Mater.* **2012**, *152*, 78–83.
64. Chiang, Y.C.; Chiang, P.C.; Chang, E.E. Effects of Surface Characteristics of Activated Carbons on VOC Adsorption. *J. Environ. Eng.* **2001**, *127*, 54–62.
65. Meininghaus, C.K.W.; Prins, R. Sorption of Volatile Organic Compounds on Hydrophobic Zeolites. *Microporous Mesoporous Mater.* **2000**, *35–36*, 349–365.
66. Dubinin, M.M. Fundamentals of the Theory of Adsorption in Micropores of Carbon Adsorbents—Characteristics of their Adsorption Properties and Microporous Structures. *Pure Appl. Chem.* **1989**, *61*, 1841–1843.
67. Mangun, C.L.; Daley, M.A.; Braatz, R.D.; Economy, J. Effect of Pore Size on Adsorption of Hydrocarbons in Phenolic-based Activated Carbon Fibers. *Carbon* **1998**, *36*, 123–129.
68. Huang, M.C.; Chou, C.H.; Teng, H.S. Pore-size Effects on Activated-carbon Capacities for Volatile Organic Compound Adsorption. *AICHE J.* **2002**, *48*, 1804–1810.
69. Brodu, N.; Zaitan, H.; Manero, M.H.; Pic, J.S. Removal of Volatile Organic Compounds by Heterogeneous Ozonation on Microporous Synthetic Alumina Silicate. *Water Sci. Technol.* **2012**, *66*, 2020–2026.
70. Lillo-Rodenas, M.A.; Cazorla-Amoros, D.; Linares-Solano, A. Behaviour of Activated Carbons with Different Pore Size Distributions and Surface Oxygen Groups for Benzene and Toluene Adsorption at Low Concentrations. *Carbon* **2005**, *43*, 1758–1767.
71. Lillo-Rodenas, M.A.; Cazorla-Amoros, D.; Linares-Solano, A. Benzene and Toluene Adsorption at Low Concentration on Activated Carbon Fibres. *Adsorption* **2011**, *17*, 473–481.
72. Li, L.; Sun, Z.; Li, H.; Keener, T.C. Effects of Activated Carbon Surface Properties on the Adsorption of Volatile Organic Compounds. *J. Air Waste Manage. Assoc.* **2012**, *62*, 1196–1202.
73. Yang, K.; Sun, Q.; Xue, F.; Lin, D. Adsorption of Volatile Organic Compounds by Metal-organic Frameworks MILL-101: Influence of Molecular Size and Shape. *J. Hazard. Mater.* **2011**, *195*, 124–131.
74. Kuroki, T.; Fujioka, T.; Okubo, M.; Yamamoto, T. Toluene Concentration Using Honeycomb Nonthermal Plasma Desorption. *Thin Solid Films* **2007**, *515*, 4272–4277.
75. Gundry, P.M.; Tompkins, F.C. Chemisorption of Gases on Metals. *Q. Rev. Chem. Soc.* **1960**, *14*, 257–291.

76. Chiang, Y.C.; Chaing, P.C.; Huang, C.P. Effects of Pore Structure and Temperature on VOC Adsorption on Activated Carbon. *Carbon* **2001**, *39*, 523–534.
77. Gregg, S.J.; Sing, K.S.W. Adsorption, Surface-area and Porosity, 2nd edition. *Text. Res. J.* **1984**, *54*, 792–792.
78. Magne, L.; Pasquiers, S. Lif Spectroscopy Applied to the Study of Non-thermal Plasmas for Atmospheric Pollutant Abatement. *C. R. Phys.* **2005**, *6*, 908–917.
79. Pringle, K.J.; Whitehead, J.C.; Wilman, J.J.; Wu, J.H. The Chemistry of Methane Remediation by a Non-thermal Atmospheric Pressure Plasma. *Plasma Chem. Plasma Process.* **2004**, *24*, 421–434.
80. Ogata, A.; Mizuno, K.; Kushiyama, S.; Yamamoto, T. Methane Decomposition in a Barium Titanate Packed-bed Nonthermal Plasma Reactor. *Plasma Chem. Plasma Process.* **1998**, *18*, 363–373.
81. Mok, Y.S.; Lee, S.B.; Oh, J.H.; Ra, K.S.; Sung, B.H. Abatement of Trichloromethane by Using Nonthermal Plasma Reactors. *Plasma Chem. Plasma Process.* **2008**, *28*, 663–676.
82. Kim, H.H.; Ogata, A. Nonthermal Plasma Activates Catalyst: From Current Understanding and Future Prospects. *Eur. Phys. J.* **2011**, *55*, 13806–13818.
83. Qu, G.; Liang, D.; Qu, D.; Huang, Y.; Li, J. Comparison between Dielectric Barrier Discharge Plasma and Ozone Regenerations of Activated Carbon Exhausted with Pentachlorophenol. *Plasma Sci. Technol.* **2014**, *16*, 608–613.
84. Kuroki, T.; Fujioka, T.; Kawabata, R.; Okubo, M.; Yamamoto, T. Regeneration of Honeycomb Zeolite by Nonthermal Plasma Desorption of Toluene. *IEEE Trans. Ind. Appl.* **2009**, *45*, 10–15.